

Article

# Study of Interfacial Adhesion between Nickel-Titanium Shape Memory Alloy and a Polymer Matrix by Laser Surface Pattern

Sneha Samal <sup>1,\*</sup>, Ondřej Tyc <sup>1</sup>, Luděk Heller <sup>1</sup>, Petr Šittner <sup>1</sup>, Monika Malik <sup>2</sup>, Pankaj Poddar <sup>2</sup>, Michelina Catauro <sup>3</sup> and Ignazio Blanco <sup>4,\*</sup>

<sup>1</sup> Institute of Physics of Czech Academy of Sciences, Na Slovance 1999/2, 182 21 Prague, Czech; tyc@fzu.cz (O.T.); heller@fzu.cz (L.H.); sittner@fzu.cz (P.Š.)

<sup>2</sup> National Chemical laboratory, Pune 411008, India; m.malik@ncl.res.in (M.M.); p.poddar@ncl.res.in (P.P.)

<sup>3</sup> Department of Engineering, University of Campania “Luigi Vanvitelli”, Via Roma 29, I-81031 Aversa, Italy; michelina.catauro@unicampania.it

<sup>4</sup> Department of Civil Engineering and Architecture and UdR-Catania Consorzio INSTM, University of Catania, Viale Andrea Doria 6, 95125 Catania, Italy

\* Correspondence: samal@fzu.cz (S.S.); iblanco@unict.it (I.B.)

Received: 22 February 2020; Accepted: 20 March 2020; Published: 23 March 2020



**Abstract:** The aim of this article is to investigate the interfacial adhesion of Ni-Ti shape memory alloy with a polymer matrix of Poly (methyl methacrylate) (PMMA). The surface pattern on Ni-Ti plates was channeled by a solid state laser machine. The laser machine allows for creating channels on the Ni-Ti surface for infiltration of the PMMA matrix, which could be attached as an intra-surface locking pattern to the Ni-Ti surface. The influence of the PMMA matrix on the surface of the NiTi plate was evaluated by thermomechanical analysis (TMA) and dynamic mechanical analysis (DMA). The surface characterization was carried out by an optical microscope on the PMMA/NiTi composite after mechanical testing. During mechanical testing, the polymer displays the multiple cracks in the longitudinal direction that result in slipping and fracture. TMA and DMA analyses were performed on the Ni-Ti- and PMMA-coated Ni-Ti ribbon to observe elasticity and the storage modulus for both samples. Better adhesion than 80 % was observed in the Ni-Ti surface, in the laser surface pattern, in comparison to the free plain surface. However, the polymer acts as mechanical backing that caused a reduction in the shape-memory properties of the composite material.

**Keywords:** adhesion; NiTi plate; polymer; PMMA/NiTi composites; mechanical properties; surface features

## 1. Introduction

The application of Ni-Ti shape memory alloys has gained considerable interest in the medical field due to the application of the pseudo elastic nature of the material in the medical devices and implants [1]. Ni-Ti shape memory alloys (SMA) are used in medical technology for applications such as stent-grafts and guide wires [2]. However, as this material of Ni-Ti-SMAs has received increased attention in the medical field due to its functional properties, the release of Ni content towards allergy issues raises serious concern for bio medical applications [3]. To avoid Ni release from Ni-Ti-SMAs, the polymer coating is gaining interest in the areas of Ni-Ti alloys. This type of application could benefit from hybrid systems like polymer-coated shape memory composites. Hybrid composites, consisting of binary or more elemental systems involving polymer and Ni-Ti, have been developed in the last 5 years [4]. Some researchers have studied polymer composite actuators with SMA alloys and taking the advantages of the glass transition temperature of the polymer and the phase transition temperature

of Ni-Ti alloys [5]. The effect of temperature on the phase transition in the hybrid composite opens up wide potential in shape setting behavior [6–9] in the field of actuators and in the mechanical response of the composite. However, the mechanical behavior of hybrid composites reveals that the interfacial adhesion between the Ni-Ti ribbon and polymer interface plays a crucial role in adhesion property, thus controlling the thermal and mechanical response of the hybrid composite [10,11]. Good adhesion between the polymer and the Ni-Ti ribbon on the surface quality holds a crucial step prior to the potential application of hybrid composites. This is because a hybrid composite of the shape memory alloy with polymer provides actuator motion with deflection, and, relying on their mechanical response, these composites of thin films are promising candidates for actuators in MEMs [12].

Ni-Ti shape memory alloys are most successful because of their good structural and functional properties and they can be combined with polymers, forming functional engineering composites (FECs). The growing demand in the sensors and actuators field could be fulfilled by FECs using shape-memory properties, such as bistable behaviour [13]. Ni-Ti shape memory alloys show thermodynamic behavior of three kinds of shape memory effect such as 1-way, 2-way, and pseudo elasticity. All shape memory effects depend on the phase transformation during high and low temperature processes. Polymeric materials are not as strong as alloys but have a number of attractive features, such as low density, good flexibility, good chemical stability, and low electrical conductivity.

Poly (methyl methacrylate) (PMMA) was chosen because of its high tensile strength and higher elastic (Young's modulus) and shear modulus of 3.2 and 1.7 GPa, respectively.

A number of parameters need to be considered prior to the composites design, including the alloy's surface conditions, the alloy's microstructure, the morphology of the polymer, the build of the metal–polymer interface, the influence of thin layers acting as a coupling agent between Ni-Ti and the polymer, the influence of different processing condition, and the influence of the thermo-mechanical load history. An alloy–polymer composite shows shape memory effect during cooling and heating. On cooling, the polymer acts as a bias spring and leads to shape change. On heating, a shape change occurs against the elastic deformation of the polymer. As a result, the composite as a whole could perform a two-way effect by reinforcing the one-way effect of Ni-Ti ribbon into the polymer matrix. The polymer matrix, in return, could act as a bias force into the material. A strong alloy–polymer interface is required to transfer the stress inside the polymer onto the shape memory alloy on cooling. The deformation of the interface during cyclic shape change in service can lead to delamination, resulting in a loss of memory. The physical nature of the polymer–alloy interface is thus a key point and a good bonding between the polymer and the shape memory alloy is required. The interaction of shape memory alloys and polymers can occur in various ranges starting from chemical to mechanical adhesion.

Research has been carried out to improve the adhesion property of Ni-Ti alloys' surface quality with polymer using silane as a coupling agent [14]. There are various methodologies to improve the interfacial adhesion, either chemically, or mechanically or using a coupling agent [15–17]. In this study, we investigate the interfacial adhesion of Ni-Ti with poly (methyl methacrylate) (PMMA) by the mechanical grooving method obtained by the laser pattern method. A mechanical test is one of the way to determine the adhesion of the polymer on the surface of the Ni-Ti ribbon. The effect of adhesion and its role towards mechanical, thermal, and physical properties have been investigated.

## 2. Experimental

### 2.1. Materials

Commercial pseudoelastic Ni-Ti ribbons, thickness 0.35 mm, with an Ni content of 50.8 % were used in this study (SAES, New Hartford, USA). Poly (methyl methacrylate) was considered here for coating material on the surface of the Ni-Ti ribbon. PMMA was chosen because of its high tensile strength and its higher elastic (Young's modulus) and shear modulus of 3.2 and 1.7 GPa, respectively. The elastic modulus of Ni-Ti ribbon in the austenite phase is 80 GPa, whilst in the martensitic phase it

is 40 GPa. Commercial powder of PMMA (Particle size: 48  $\mu\text{m}$ , M.W: 550 kg/mol) was purchased from Sigma-Aldrich. A solid state laser RD 20 was used for mechanical surface grooving on the Ni-Ti surface.

## 2.2. Methods

The thermo-mechanical response of the composite was investigated by thermo-mechanical analysis (TMA) by using a LINSEIS L75 Cryo (Linseis, Sel, Germany) to observe the deflection in terms of displacement during the cooling and heating profiles. The displacement of the Ni-Ti ribbon and its corresponding composite, on one and both sides, were considered at a constant load of 200 mN with a strain rate of 0.01 m/s. The temperature was chosen in the range of  $-150\text{ }^{\circ}\text{C}$  to  $+150\text{ }^{\circ}\text{C}$ .

Dynamical mechanical analysis (DMA) was used to investigate the effect of temperature, stress, and frequency on the mechanical response of the Ni-Ti ribbon and its corresponding thermos-elastic transformation. An 8000 Perkin Elmer DMA machine was employed to carry out the test with a frequency of 0.1 Hz and a heating and cooling rate of 2 K/min in the temperature range of  $-150\text{ }^{\circ}\text{C}$  to  $+150\text{ }^{\circ}\text{C}$ .

Differential scanning calorimetry (DSC) analysis was carried out by a Pyris Diamond DSC (Perkin Elmer) for the determination of the phase transition and glass transition temperature, respectively. The sample was heated at  $10\text{ }^{\circ}\text{C}/\text{min}$  from room temperature up to  $180\text{ }^{\circ}\text{C}$ , and then maintained for one minute at this temperature before starting with cooling at the same scanning rate. At the phase transformation temperature, the Austenitic ( $A_s$ ) and Martensitic ( $M_s$ ) peaks were identified as  $-7.1\text{ }^{\circ}\text{C}$  and  $-59.5\text{ }^{\circ}\text{C}$ , respectively (Figure 1).

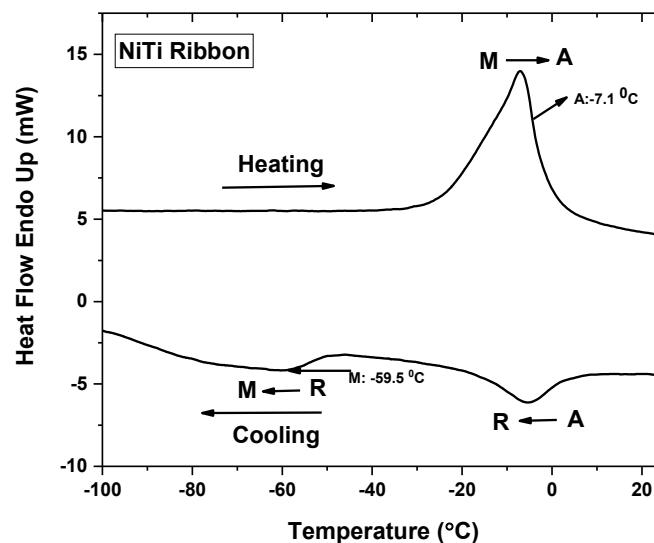


**Figure 1.** Phase transformation temperature of Ni-Ti ribbon with austenitic ( $A_s$ ) and martensitic ( $M_s$ ) phases.

The glass transition temperature ( $T_g$ ) for the PMMA was  $66.7\text{ }^{\circ}\text{C}$ , with a specific heat capacity of  $C_p$ :  $0.32\text{ J/g }^{\circ}\text{C}$  (Figure 2).

The tensile behavior of the composite and its components was evaluated by means of an E10K Instron machine (Instron, Norwood, MA, USA), with strain controlled mode. The strain rate was chosen at 0.01% S with the steps of the loading and unloading stage. The stress vs. strain curves of the Ni-Ti ribbon and its hybrid composite were obtained at room temperature. The surface features of the composite, and the corresponding adhesion of the polymer on the Ni-Ti surface, was examined by a Zeiss Imager Z1 Optical Microscope (Zeiss, Oberkochen, Germany).

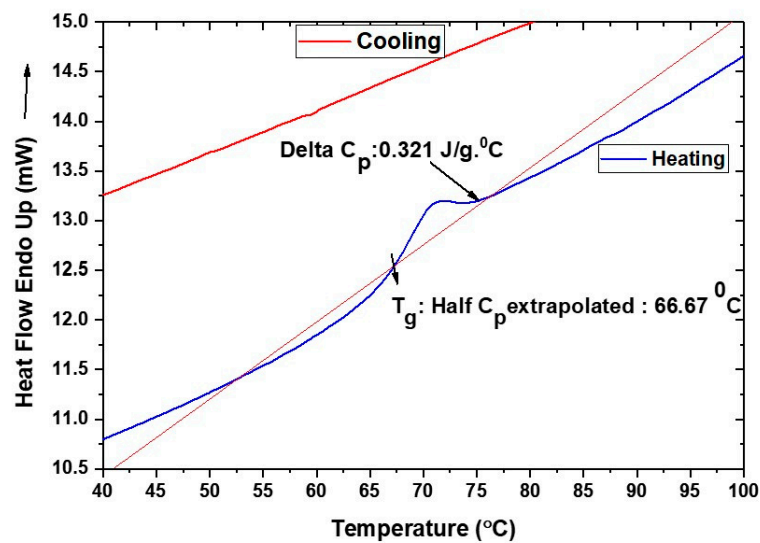


**Figure 2.** Differential scanning calorimetry curves: the blue color for heating poly (methyl methacrylate), and the red color one for cooling poly (methyl methacrylate).

The pseudoelastic Ni-Ti ribbons (cold rolled, straight annealed), with cross sectional dimensions of  $0.35 \times 30$  mm, were prepared from the plate of dimension  $300 \times 300$  mm by laser cutting. The surface of the Ni-Ti ribbon was patterned by laser engraving, with variable depth, using various power sources, such as laser heat and scanning speed. The effect of laser fluency energy was 20% of the maximum power 4 W, with a frequency of 20 kHz and a laser of 100 ns pulse length along the length of the Ni-Ti ribbon. The aim of the laser pattern was to provide a channel for polymer infiltration, thus generating a better interface between the coating layer with the interlock mechanism.

Spin coating has been considered as an efficient technique for the deposition of the polymer, such as natural rubber, polystyrene, and poly (methyl methacrylate) in very thin films on a flat surface [16]. The intensity of the laser beam with respect to the depth of the channels is reported in Figure 3, showing the laser pattern surface of Ni-Ti and the Gaussian profile distribution of the laser beam considered for engraving the channels on the surface.

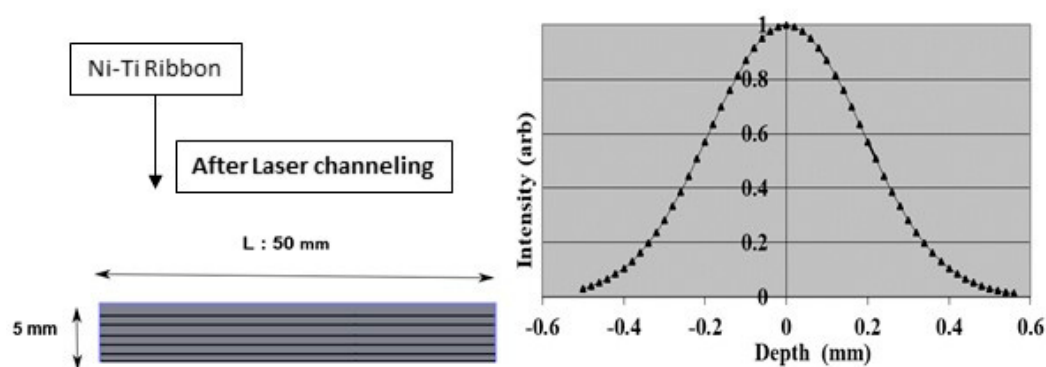


**Figure 3.** Channel on the Ni-Ti ribbon and its laser intensity versus depth of the Gaussian profile for the surface pattern.

The spin coating of PMMA on the surface of Ni-Ti ribbon was carried out using a standard spin coater (Spin Coater, Germany, Model No. SUSS MicroTec Lithography GmbH, Type DELTA 10 IT, Germany). PMMA powder was diluted with toluene (Sigma Aldrich) in the ratio of 1:10 for a concentrated solution. The suspension of the PMMA powder and solvent underwent stirring using a magnetic stirrer for 12 h at room temperature. The prepared solution was used for the coating of Ni-Ti ribbon in the spin coater for the homogenized coating of the composite. Figure 4 displays the scheme of

the spin coater, the inner view shows the holder for substrate in position using a vacuum chuck, and the motor allows the rotation of the sample after the polymers are in the position of the Ni-Ti ribbon.

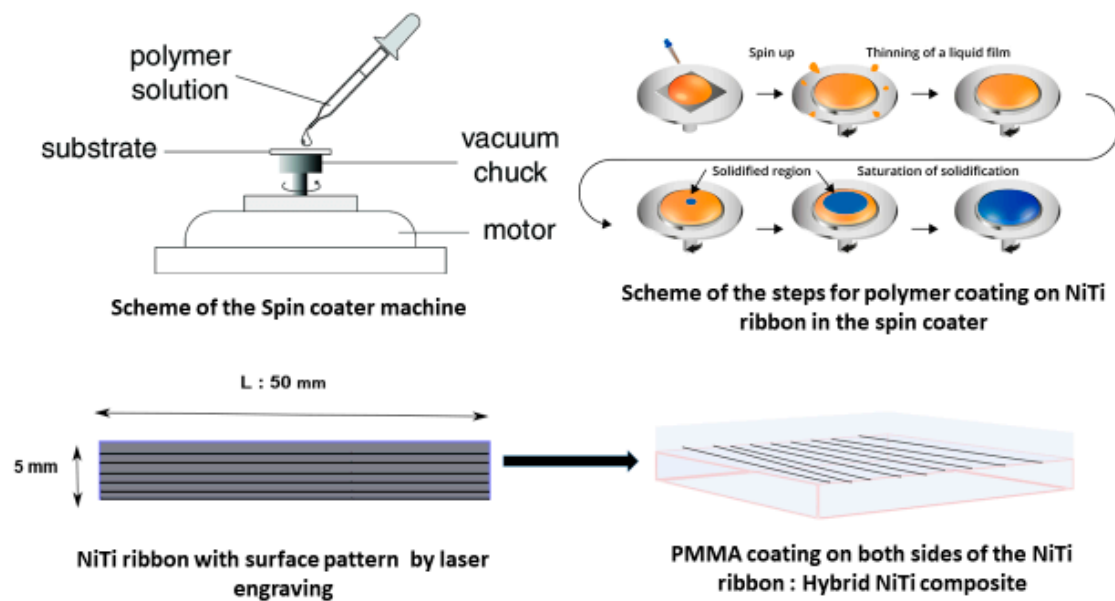


**Figure 4.** Scheme of the Ni-Ti ribbon with channels and poly (methyl methacrylate) (PMMA) polymer by spin coating.

The rotation's speed was controlled and chosen for a certain interval of time for a uniform distribution of the polymer on the surface of the Ni-Ti ribbon. After the deposition, the polymer solidifies on the substrate and the hybrid composite undergoes curing at 60 °C inside the vacuum furnace overnight. A batch of composite samples was prepared to choose various RPM, on the one side and both sides surface, for interface analysis and mechanical response. Furthermore, a batch of the composite coated on the virgin Ni-Ti samples, without laser lines, was prepared by spin-coating. The residence time was chosen 5 and 2 times to maintain the thicker and thinner coating layers with the alternative one side and both sides of the ribbon. After spin coating, the samples underwent curing at 60 °C inside the vacuum furnace overnight. Table 1 shows the specification of the composite prepared by the spin coater.

**Table 1.** Specification of the various samples obtained by spin coating: the speed of the substrate ( $v$ ); the coating surface (CS); the residence time ( $t_r$ ) of the coating; the number of the coating layer (CL); the coating thickness  $d$  ( $\mu\text{m}$ ); the quality.

Samples	$v$ /(RPM)	CS	$t_r$ /min	CL	$d$ /( $\mu\text{m}$ )	Quality
1	Ni-Ti ribbon with the channel of the engraved line without any coating					
2	100	One side	7	4 times (one surface)	0.18	Good
3	200		5	3 times (one surface)	0.17	Medium
4	300		2	2 times (one surface)	0.15	×
5	100		7	2 × 4 times	0.36	Good
6	200	Both Sides	5	2 × 3 times	0.34	Medium
7	300		2	2 × 2 times	0.30	×

### 3. Results and Discussion

#### 3.1. Micro Structural Characterization of the Composite of the Ni-Ti ribbon and Polymer

First, PMMA was spin coated on the Ni-Ti ribbon surface without the laser channel, showing complete detachment after curing. With a thick polymer's coating layer, there is delamination



of the polymer from the surface that leads to a complete separation of the polymer layer from the surface of the Ni-Ti ribbon. Otherwise, a thin coating layer results in the peeling off of the polymer in the localized area from the Ni-Ti ribbon after curing (Figure SM1). The optical images of the Ni-Ti ribbon surface were taken before and after the spin coating was examined for the adhesion. The surface of the Ni-Ti ribbon was smooth without any distortion. After the laser channel, the polymer was introduced into the surface of the Ni-Ti ribbon by the spin-coating method. The surface of the composite was examined, which showed the adhesion of the polymer into the channel that holds the polymer effectively. Figure 5 shows the Optical Micrograph (OM) images of the Ni-Ti ribbon surface and the composite after PMMA infiltrates into the channel.

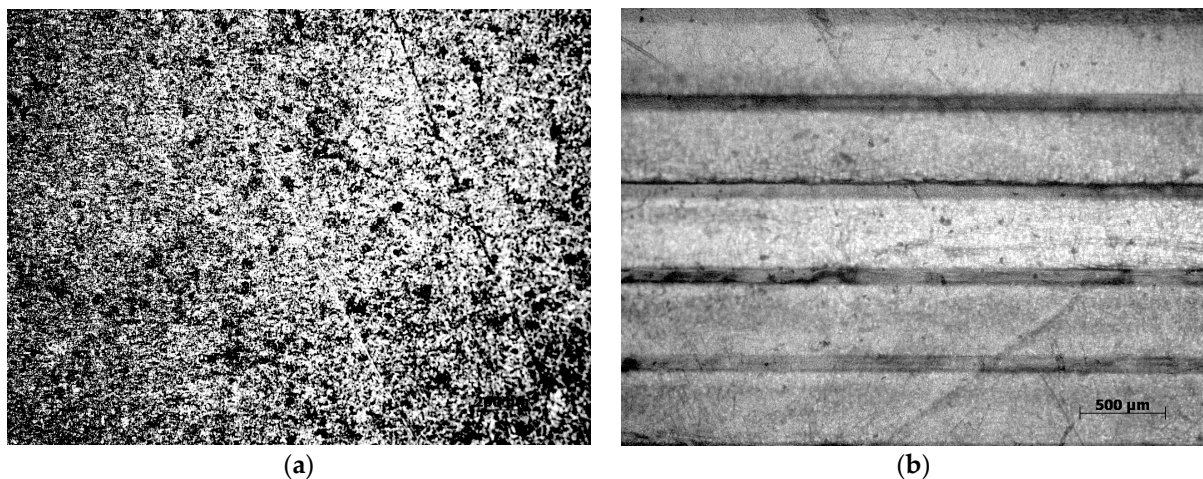


**Figure 5.** Optical Micrograph (OM) images of the (a) Ni-Ti ribbon and (b) poly (methyl methacrylate)-Ni-Ti ribbon composite.

### 3.2. Thermo-Mechanical Characterization of Composite

The thermo-mechanical response of the prepared materials was investigated by TMA to observe the deflection in terms of displacement during the cooling and heating profile. In the investigated range ( $-150$ – $150$  °C), Ni-Ti ribbon displayed the deflection ( $L$ ) in the maximum range of  $-1200$  mm; however, on the coating of the polymer to one side, the surface leads to a deflection decrease towards  $-350$  mm. This decrease in the behavior of the deflection contributes towards additional load in the three-point bending test.

The decrease in deflection behavior was more significant after the coating on both sides, probably because on cooling and heating ranges polymer has significantly adhered to the substrate without any delamination or breakage.

Figure 6 reports the deflection behavior in  $\Delta L$  as a function of the temperature and time for the Ni-Ti ribbon and PMMA composites, based on the definition of the coefficient of thermal expansion (CTE), it is clear that a large value corresponds to a phase change in the material. The change in the displacement of the Ni-Ti ribbon compared to composite shows a large difference due to the presence of the polymer coating on the surface of the alloy. The polymer coating acts as a back force, showing the good adhesion of the polymer during the heating and cooling cycles.

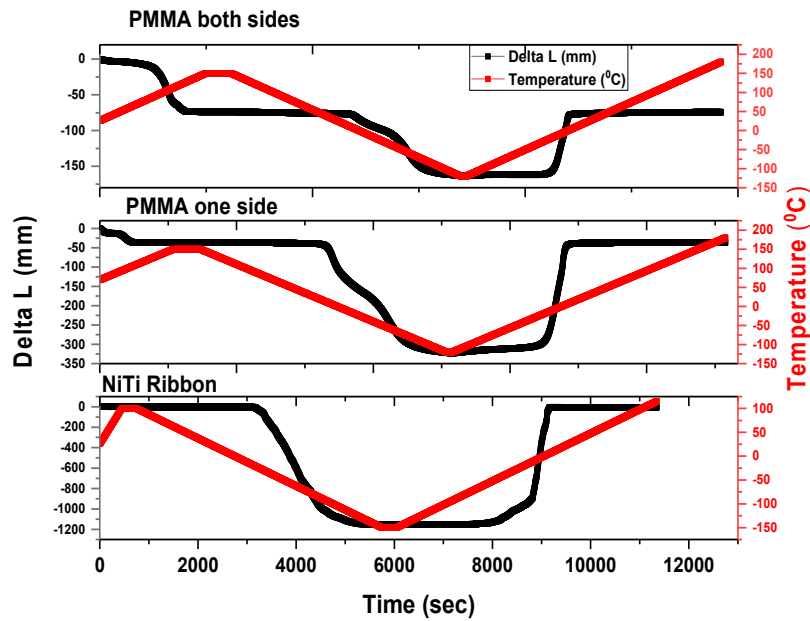


Figure 6. Displacement as a function of time and temperature for the Ni-Ti ribbon and PMMA composite.

The behavior of the hysteresis curve for the composite showed no significant difference in respect of the coating thickness on the one side and both side samples. The coefficient of thermal expansion remains unchanged for both of the composites. Figures 7 and 8 display the response of the Ni-Ti ribbon and composite as a function of the temperature and their corresponding expansion, respectively. The values are significantly reduced from the Ni-Ti ribbon. The polymer still sustains, during cooling and heating cycles, without any delamination from the Ni-Ti surface. The heating profile shows the combination of the austenite and martensitic peaks; as a result, a bi-furcated peak has been observed. On the cooling segment, the austenite and martensitic peaks, with the conversion from B<sub>2</sub> to R, and the B1<sub>9</sub>' combined peaks are observed. For the Ni-Ti ribbon–polymer composite, the values of the displacement (*L*) reduce in comparison to the Ni-Ti ribbon as a virgin sample response (Figure 7). As mentioned before, the polymer acts as a load to the Ni-Ti surface, which could backlog force.

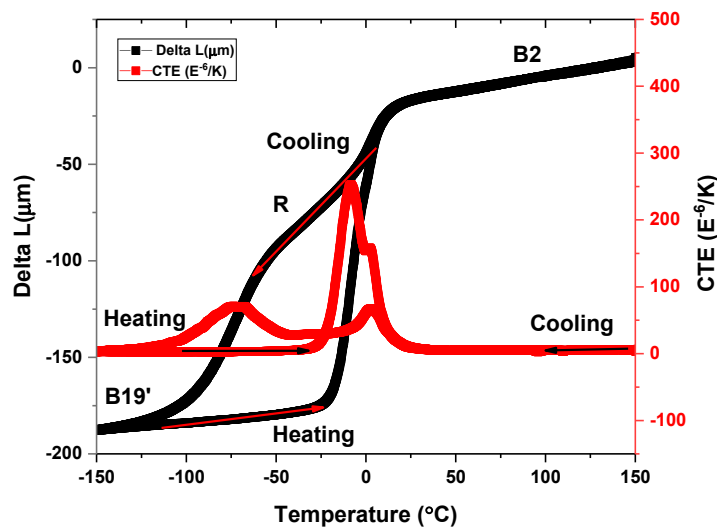


Figure 7. Thermomechanical analysis (TMA) curves of the Ni-Ti ribbon showing displacement (*L*) and the coefficient of thermal expansion (CTE) versus the temperature profile.

The thickness of the composite increases with the load applied on the surface, and, as a result, the displacement response reduces. The rule of mixture applies here as the combined effect from the matrix polymer as well as the ribbon (Figure 8).

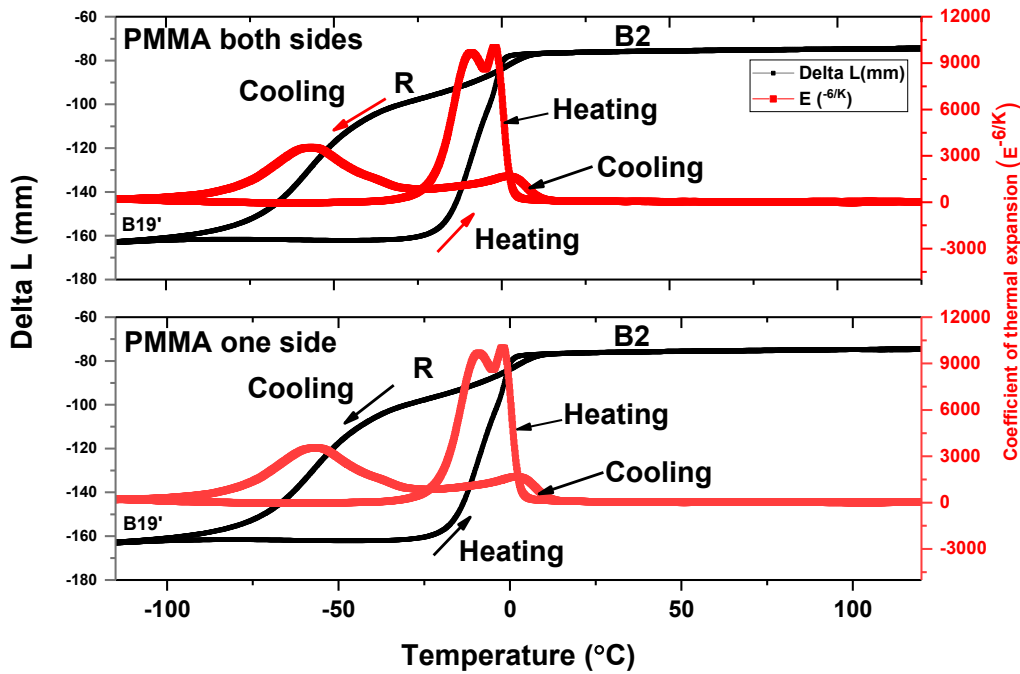


Figure 8. Hysteresis behavior of the PMMA-Ni-Ti composite (one side and both sides) surface as a function of the temperature.

The coefficient of thermal expansion (CTE) of the PMMA composite with one side showed the lower effect of PMMA on the functional behavior of the shape memory alloy (Figure 9).

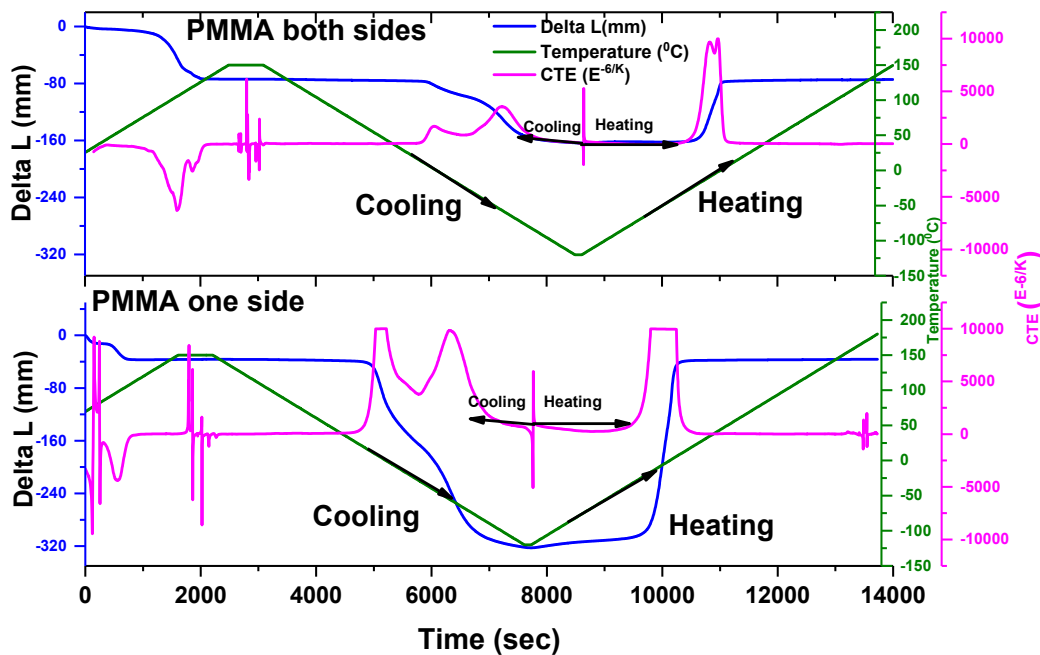


Figure 9. The coefficient of thermal expansion (CTE) response of the composite as a function of time.



The peaks are more prominent during the cooling and heating segment. However, the coating of PMMA on both sides of the Ni-Ti ribbon induces some mechanical effects, and, as a result, the peaks are less prominent during the heating and cooling segment. The mechanical behavior of the composite during cooling and heating shows no delamination of the coating from the substrate.

### 3.3. Dynamical Mechanical Characterization of the Composite

The effect of temperature, stress, and frequency on the mechanical response of the Ni-Ti ribbon and its corresponding thermo-elastic transformation was evaluated by DMA in the temperature range of  $-150\text{ }^{\circ}\text{C}$  to  $+150\text{ }^{\circ}\text{C}$ .

Figure 10 shows the DMA response of the Ni-Ti ribbon and the corresponding hybrid composite. The storage modulus and  $\text{Tan } \delta$  of the prepared materials were determined as a function of the temperature. The  $\text{Tan } \delta$  value corresponds to the internal friction of the sample, which is calculated from the dissipated energy of the sample ( $E'$ ) to the ratio of the storage modulus ( $E''$ ) of the material. The transformation temperatures from the martensitic phase ( $B_{19'}$ ) to the austenitic one ( $B_2$ ), during the heating of the Ni-Ti ribbon, and from the austenitic to the martensitic phase, during the cooling of the Ni-Ti ribbon, are depicted from the Figure 10.

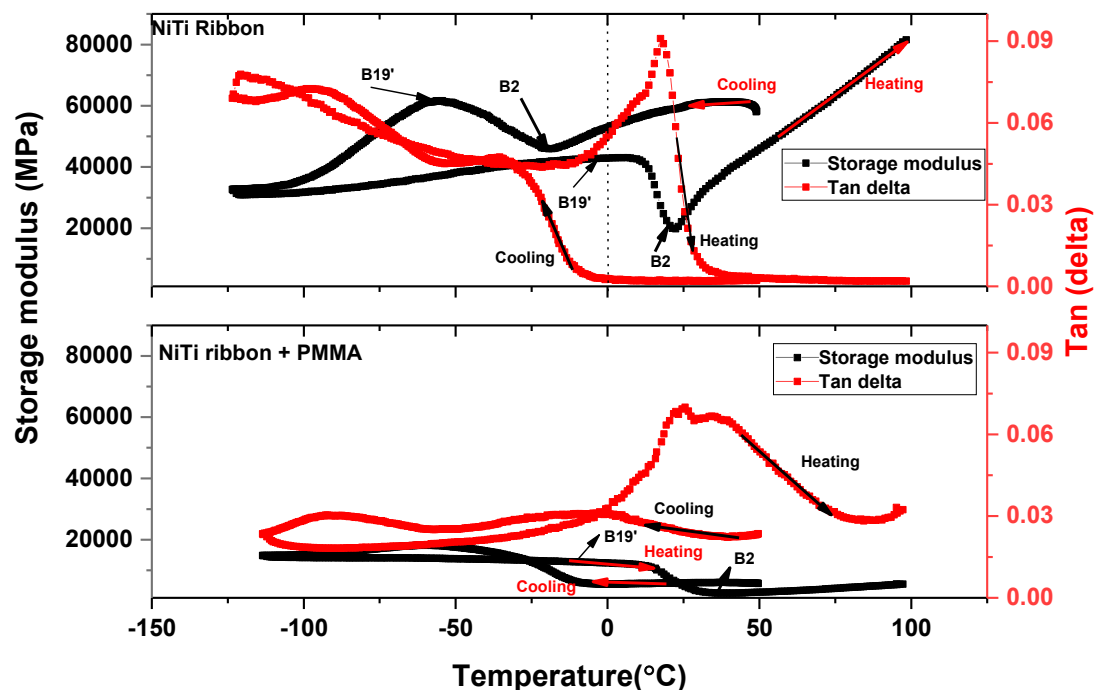


**Figure 10.** Dynamic mechanical analysis (DMA) response of the Ni-Ti ribbon and PMMA Ni-Ti ribbon composite.

The polymeric matrix showed the high damping and low modulus in comparison to the higher value of the modulus of the Ni-Ti ribbon. The DMA of the composite showed the combination of the effect of the Ni-Ti ribbon and polymer. As the Ni-Ti ribbon and polymer showed the reverse effect in their response, the composite showed the predominate behavior of the polymer with reduced storage modulus and  $\text{Tan } \delta$  values. The presence of the polymer was confirmed from the reduced hysteresis response of the Ni-Ti ribbon–polymer composite. The heating–cooling profile of the Ni-Ti ribbon–PMMA for the storage modulus showed the transformation of  $B_{19'}$  to the  $B_2$  phase with a reduced hysteresis area. This draws attention to the fact that the laser line promotes an increase in surface area by creating a channel for better adhesion into the valley of the Ni-Ti surface. This improves adhesion during the interlocking of the polymer into the depth of the channel without any chemical interaction between the Ni-Ti ribbon or polymer.

### 3.4. Tensile Study of the Ni-Ti Ribbon and Composite

The tensile study of the Ni-Ti ribbon and its corresponding composite were carried out in an Instron machine using the strain-controlled mode at room temperature (Figure 11). The stress of 400 MPa was reached at the strain of 8% with the transformation of the austenitic to martensitic super elastic plateau upon loading and the martensitic to austenitic phase upon unloading with an un-recovered strain of 0.1%. However, the composite with one surface coating showed a reduction in the stress of 280 MPa with a strain of 4.8% upon loading, with a similar value for the un-recovered strain of 0.1%. The composite with the both-side PMMA coating displayed the stress of 220 MPa with a strain of 3.5%. The composites and Ni-Ti ribbon recovered back to their original shape after unloading with an un-recovered strain of 0.1%. The interface of the polymer with the Ni-Ti ribbon was then examined after the tensile test.

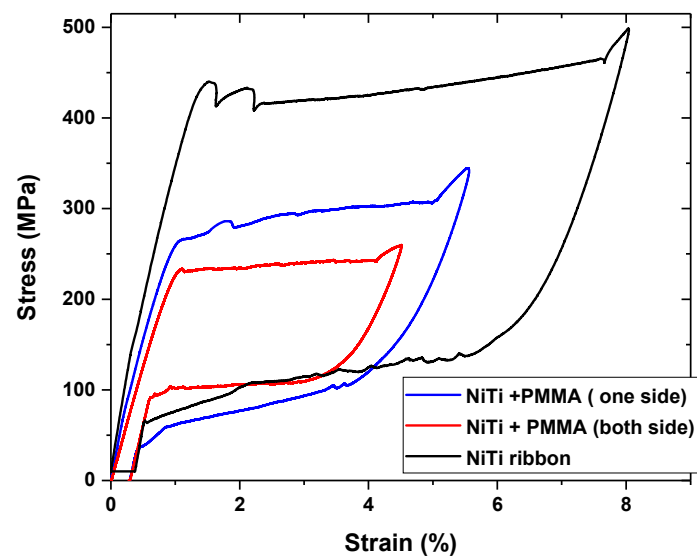


**Figure 11.** Stress–strain curves for the Ni-Ti ribbon and its corresponding hybrid composite.

### 3.5. Micro Structural Characterization of the Polymer-Ribbon Interface after the Tensile Test

The adhesion of the polymer on the Ni-Ti ribbon surface after the tensile test was examined by optical microscopy. The surface image of the composite after the tensile test shows that the adherence of the polymer still holds good on the surface of the Ni-Ti ribbon. In Figure 12a–d, it is possible to observe the various regions of the composite’s surface after the tensile test. Figure 12a shows the transverse direction of the polymer tearing up during the tensile test. Notwithstanding this, the adhesion remains constant across the surface of Ni-Ti ribbon. Figure 12b shows the tearing of the polymer from both edges in the transverse direction towards the surface of the composite. Figure 12c shows the clamping area and its surroundings. The clamping zone shows the rupture of the polymer from the Ni-Ti alloy surface; however, the close area shows a transverse crack line along the surface of the composite. Figure 12d displays the image of transverse and longitudinal cracks along the surface of the composite. During the tensile test, although some cracks and the tearing of the polymer were exhibited, the adhesion is still very compatible. The polymer was completely un-detached from the surface, thus confirming that the adhesion of the polymer on the surface of the Ni-Ti ribbon still displays good results.

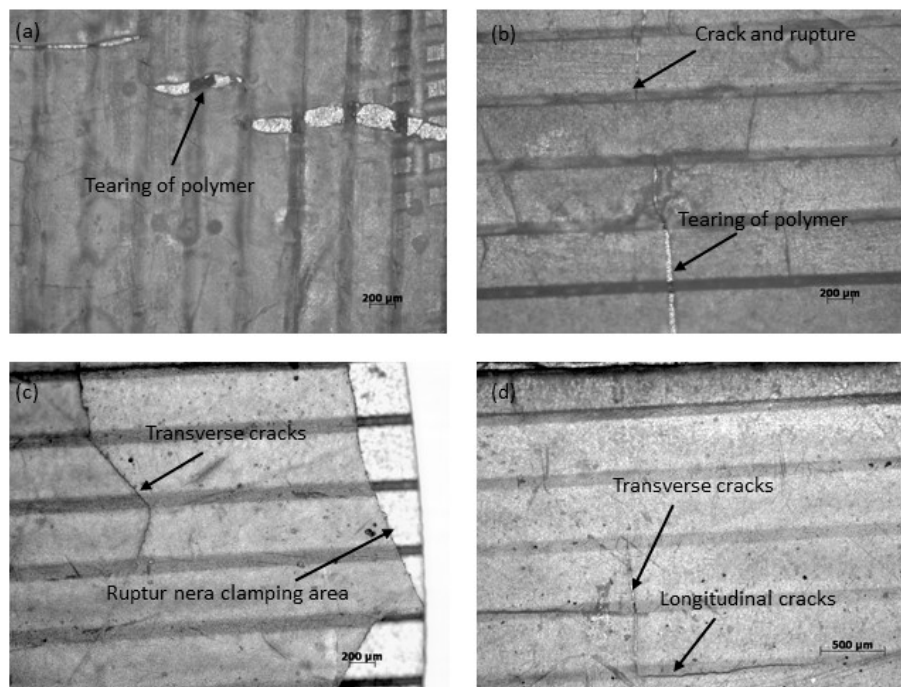


**Figure 12.** Optical microscopy surface images of the PMMA composite after the tensile test.

The mechanical roughness created by the laser beam on the surface of the Ni-Ti ribbon stands well in the adhesion of the polymer on the Ni-Ti ribbon surface. The channels provide a good path for the infiltration of the polymer onto the surface, providing, in the meantime, a valley of polymer intact towards the surface with the interlocking mechanism of the two material.

#### 4. Conclusions

A hybrid composite material exhibits better adhesion of the polymer on the Ni-Ti ribbon surface by applying mechanical roughness to the surface. In this work, mechanical roughness was created by laser engraving the surface of the Ni-Ti ribbon. The channel allows for the infiltration of the polymer matrix into the surface of the Ni-Ti ribbon. This interlocking mechanism of the polymer into the alloy surface provides stronger interfacial adhesion of the polymer without any breakage. The composite showed improved adhesion behavior in comparison to the starting material. However, the polymer induces backlog on the performance of the mechanical response of the material. A better adhesion of the polymer on the Ni-Ti surface may improve the composite properties in the areas of the sensors and actuators on controlling the movement during thermal cycles. The cooling and heating cycles induce the hardening and softening mechanism of the polymer that adheres to the Ni-Ti surface. The composite behavior reflects on the combination of the mechanism of the polymer and the Ni-Ti ribbon under thermal cycles. Mechanical tests were also performed to observe the adhesion of the polymer into the channel of the Ni-Ti surface. During good adhesion, the composite could act, as in the field of actuators, using shape memory effect rather than mechanical strength. The bending and shape recovery of the composite as the function of heating and cooling temperature could stand as a potential technique in the transducer and actuator field of application.

**Supplementary Materials:** The following are available online at <http://www.mdpi.com/2076-3417/10/6/2172/s1>, Figure SM1: Images of the polymer PMMA on Ni-Ti surface without laser lines showing a detachment from the surface.

**Author Contributions:** S.S., P.S. and I.B. conceived and designed the study; M.M. and P.P. performed the experiments; Discussion on article write up and necessary modification was carried out by all the authors in a team effort. All authors have read and agreed to the published version of the manuscript.

**Funding:** This work was carried out within the Institute of Physics and Institute of Plasma Physics under the Solid-21 project (SOLID21: CZ.02.1.01/0.0/0.0/16\_019/0000760, SOLID21-Fyzika pevných látek pro 21. Století, Fyzikální ústav AV ČR, v. v. i. (2018–2023). Ignazio Blanco is grateful to the University of Catania within the “Bando-CHANCE” n° 59722022250, for supporting the project HYPERJOIN-HYBRID HIGH PERFORMANCE INNOVATIVE JOINTS.

**Conflicts of Interest:** The authors declare no conflict of interest.

## References

1. Saburi, T. Ti-Ni shape memory alloys. In *Shape Memory Materials*; Otsuka, K., Waymann, C.M., Eds.; Cambridge University Press: Cambridge, UK, 1999; pp. 49–96. ISBN 9780521663847.
2. Kapoor, D. Nitinol for medical applications: A brief introduction to the properties and processing of nickel titanium shape memory alloys and their use in stents. *Johns. Matthey Technol. Rev.* **2017**, *61*, 66–76. [[CrossRef](#)]
3. Ryhänen, J.; Niemi, E.; Serlo, W.; Niemelä, E.; Sandvik, P.; Pernu, H.; Salo, T. Biocompatibility of nickel-titanium shape memory metal and its corrosion behavior in human cell cultures. *J. Biomed. Mater. Res.* **1997**, *35*, 451–457. [[CrossRef](#)]
4. Lomas-González, O.; López-Cuellar, E.; López-Walle, B.; José de Araujo, C.; Reyes-Melo, E.; Gonzalez, C.H. Thermomechanical behavior of a composite based on a NiTi ribbon with a magnetic hybrid polymer. *Mater. Today Proc.* **2015**, *2*, S785–S788. [[CrossRef](#)]
5. López-Walle, B.; López-Cuellar, E.; Reyes-Melo, E.; Lomas-González, O.; De Castro, W.B. A Smart Polymer Composite Based on a NiTi Ribbon and a Magnetic Hybrid Material for Actuators with Multiphysic Transduction. *Actuators* **2015**, *4*, 301–313. [[CrossRef](#)]
6. Samal, S.; Heller, L.; Brajer, J.; Tyc, O.; Kadrevik, L.; Sittner, L. Laser Annealing on the Surface Treatment of Thin Super Elastic NiTi Wire. *IOP Conf. Ser. Mater. Sci. Eng.* **2018**, *362*, 012007. [[CrossRef](#)]
7. Samal, S.; de Prado, E.; Tyc, O.; Sittner, P. Shape Setting in super-elastic NiTi ribbon. *IOP Conf. Ser. Mater. Sci. Eng.* **2019**, *461*, 012075. [[CrossRef](#)]
8. Samal, S.; de Prado, E.; Manak, J.; Tyc, O.; Heller, L.; Sittner, P. Internal stresses and plastic strains introduced into surface layers of bent NiTi ribbon by low temperature shape setting. In Proceedings of the ASM International-International Conference on Shape Memory and Superelastic Technologies, Konstanz, Germany, 13–17 May 2019; pp. 100–101. ISBN 978-151089272-9.
9. Samal, S.; Heller, L.; Brajer, J.; Manak, J.; Sittner, P. Gradient of hardness and Young’s modulus over crosssection of laser annealed NiTi wires. *Esmat Proc.* **2018**, *362*, 012007.
10. Samal, S.; Stuchlík, M.; Petrikova, I. Thermal behavior of flax and jute reinforced in matrix acrylic composite. *J. Therm. Anal. Calorim.* **2018**, *131*, 1035–1040. [[CrossRef](#)]
11. Samal, S.; Škodová, M.; Blanco, I. Effects of Filler Distribution on Magnetorheological Silicon-Based Composites. *Materials* **2019**, *12*, 3017. [[CrossRef](#)] [[PubMed](#)]
12. Tobushi, H.; Hayashi, S.; Pieczyska, E.; Date, K.; Nishimura, Y. Three-way actuation of shape memory composite. *Arch. Mech.* **2011**, *63*, 443–457.
13. Chillara, V.S.C.; Dapino, M.J. Shape memory alloy-actuated bistable composites for morphing structures. *SPIE Proc.* **2018**, *10596*, 1–8. [[CrossRef](#)]
14. Smith, N.A.; Antoun, G.G.; Ellis, A.B.; Crone, W.C. Improved adhesion between a nickel-titanium shape memory alloy and a polymer matrix via silane coupling agents. *Compos. Part A Appl. Sci. Manuf.* **2004**, *35*, 1307–1312. [[CrossRef](#)]
15. Ehrenstein, G.W. *Polymeric Materials. Structure, Properties, Applications*. Hanser, Munich; Carl Hanser Verlag: Munich, Germany, 2004; ISBN 978-3-446-21461-3.
16. Wingfield, J.R.J. Treatment of composite surfaces for adhesive bonding. *Int. J. Adhes. Adhes.* **1993**, *13*, 151–156. [[CrossRef](#)]
17. Extrand, C.W. Spin coating of very thin polymer films. *Polym. Eng. Sci.* **1994**, *34*, 390–394. [[CrossRef](#)]

